Estimation of Gas Permeability of a Zeolite Membrane, Based on a Molecular Simulation Technique and Permeation Model

Shigejirou Suzuki, Hiromitsu Takaba,* Takeo Yamaguchi, and Shin-ichi Nakao

Department of Chemical System Engineering, Graduate School of Engineering, The University of Tokyo, 7-3-1 Hongo, Bunkyo-ku, Tokyo 113-8656, Japan

Received: July 21, 1999; In Final Form: December 2, 1999

A method for estimating gas permeability through a zeolite membrane, using a molecular simulation technique and a theoretical permeation model, is presented. The estimate of permeability is derived from a combination of an adsorption isotherm and self-diffusion coefficient based on the adsorption-diffusion model. The adsorption isotherm and self-diffusion coefficients needed for the estimation were calculated using conventional Monte Carlo and molecular dynamics simulations. The calculated self-diffusion coefficient was converted to the mutual diffusion coefficient and the permeability estimated using the Fickian equation. The method was applied to the prediction of permeabilities of methane and ethylene in silicalite at 301 K. Calculated permeabilities were larger than the experimental values by more than an order of magnitude. However, the anisotropic permeability was consistent with the experimental data and the results obtained using a grand canonical ensemble molecular dynamics technique (Pohl et al. *Mol. Phys.* **1996**, *89* (6), 1725−1731).

1. Introduction

Recently, much attention has been given to the preparation of zeolite membranes so as to obtain optimal use of their molecular sieving and adsorption properties. Numerous experimental studies on the performance of zeolite membranes for selective permeation of gases or liquids have been reported.[1−4] It has still been difficult, however, to determine experimentally the absolute value of permeability, and the type of zeolite membrane most suitable for a particular separation system, because the performance of a zeolite membrane is greatly dependent on the conditions of its synthesis, and thus on the structure obtained. Therefore, some theoretical methodology based on a physical model was required to predict the performance of a zeolite membrane and to design a suitable membrane for a particular separation system.

In recent years, there have been several computer simulation studies[5−10] on adsorption and diffusion of molecules inside zeolite, based on accurate intermolecular potentials. They have focused mainly on intracrystalline diffusion in the absence of a concentration gradient. However, there have been studies[11−16] that treated the transport in membranes with a concentration gradient. The majority of these studies used a grand canonical ensemble molecular dynamics (GCMD) technique, because nonequilibrium conditions could be simulated directly. The applicability of this method is limited due to time restrictions imposed by the central processing unit (CPU); for example, the simulated membrane thickness is limited to a few nanometers at most, whereas the actual membrane thickness is a few micrometers. An increase in membrane thickness clearly means an increase in the number of atoms considered, and consequently the computing time increases dramatically. Although the GCMD technique is a powerful tool giving insight into the dynamics of permeation in a membrane, an alternative approach is required for predicting the performance of a membrane.

* Corresponding author. Phone:+81-3-5841-8839. Fax:+81-3-5841-7279. E-mail: takaba@nakao1.t.u-tokyo.ac.jp.

The method presented here, using equilibrium simulation techniques, assumes the diffusion−adsorption model. This model postulates that the motion of a permeating molecule is described by a sequence of jumping-like diffusion from one adsorption site to a neighboring adsorption site. Theoretical studies based on this model include Kapteijn et al.,[17] who calculated permeance of light hydrocarbon through a silicalite membrane using the generalized Maxwell−Stefan equations; their calculated permeances agreed well with the experimental data. Vroon et al.[18] tried to explain the temperature dependence of permeance for *n*-butane through a silicalite membrane, assuming that the temperature dependence of diffusion coefficients obeyed the Arrhenius equation. Recently, Krishna et al.[19,20] used Maxwell−Stefan theory to demonstrate the possibility of separating the hydrocarbon isomers across a silicalite membrane, and estimated the Langmuir parameters necessary for the calculation using the configurational-bias Monte Carlo method. However, they did not give any discussion of how the mutual diffusion coefficient was obtained using molecular simulation technique. Fritzsche et al.[14] estimated the mutual diffusivity from the MD results and confirmed that they agreed well with experimental NMR (nuclear magnetic resonance) results. Fried et al.[21] estimated the permeability of small molecules across a polymer membrane, from diffusion coefficients and a solubility factor, which were calculated from MD simulations. To our knowledge, there have been no studies estimating the permeability of zeolite membranes based on the results of molecular simulation techniques.

In this paper, we have tried to estimate the permeability of zeolite membranes, using a diffusion−adsorption model and molecular simulation techniques, and to apply them to the permeability calculations of ethylene and methane in silicalite.

2. Permeability Calculation

An estimate of permeability, in the zeolite membrane considered here, is possible by using a specific assumption. In this section, we present the theoretical background. The relation-

10.1021/jp992521i CCC: $19.00
Published on Web 02/15/2000

ship between the transport diffusion coefficient, D, and the thermodynamically corrected diffusion coefficient, D_0, is known as the "Darken equation" and is given by

$$D = D_0 \frac{\partial \ln p}{\partial \ln q}$$

where p is the pressure of the adsorbate and q is the amount of adsorption.

Many studies have assumed that the corrected diffusion coefficient and the self-diffusion coefficient, D_s, are equal,[22−24] but the agreement is seen only in the limit of an infinitely dilute adsorbate system.[12] In this study, we distinguish between these two coefficients and formulate a relationship between them. Using the Maxwell−Stefan diffusivity,[25] it is possible to obtain a relationship between the self-diffusion and transport diffusion coefficients, given by

$$D_s = \frac{D'_{12} D'_1}{\theta D'_1 + (1-\theta) D'_{12}} \tag{1}$$

$$D_0 = D'_1 = \frac{D'_{1,n+1}}{(1-\theta)} = \frac{D'_{1v}}{(1-\theta)} \tag{2}$$

$$D = D_0/(1-\theta) \tag{3}$$

where D'_{12} and D'_{1v} are the Maxwell-Stefan diffusion coefficients, θ is the site occupancy, D'_{1v} represents the facility for molecules to jump to a vacant site, and D'_{12} represents the facility for counterchanges; that is, the adsorbed species 2 is replaced by the adsorbed species 1 at an adsorption site. Both D'_{12} and D'_{1v} are dependent on concentration. Consequently, it is impossible to calculate them exactly by using only the concentration dependence of the self-diffusion coefficient.

Various formulations, based on a physical model, have been proposed for the concentration dependence of the corrected diffusivity, D_0. Krishna et al.[26,27] correlated the concentration dependence of D'_1 with the D'_{1v} as follows:

$$D'_{1v} = \frac{1}{2}\lambda^2 \nu(\theta) \tag{4}$$

where λ is the mean displacement and υ is the jump frequency of adsorbed species at θ site occupancy. Suppose that a molecule can migrate from a certain site to a nearest neighbor vacant site, the jump frequency of adsorbed species is proportional to $(1-\theta)$, and D'_{1v} is found to be

$$D'_{1v} = \frac{1}{2}\lambda^2 \nu(\theta) = D'_{1v}(0)(1-\theta) \tag{5}$$

We can now estimate the transport diffusion coefficient, D_0, using the self-diffusion coefficient, D_s, as follows:

$$D_0 = D'_{1v}(0) = \lim_{\theta \to 0} D_s(\theta) \tag{6}$$

Using eqs 1−6, the transport diffusivity, D, can be derived from the value of D'_{1v} at zero occupancy. In the limit of an infinitely dilute adsorbate region, the interaction between the molecules becomes insignificant so that the dependence of D'_{1v} on the concentration can be considered to be equal to that of the self-diffusion coefficient. Therefore, we estimated D_0 by a linear fit of self-diffusion coefficients (obtained from MD calculations) in the low occupancy region.

The flux of diffusing species was calculated using the Fickian equation, and was given by

$$J = -D\frac{dq}{dx} \tag{7}$$

where x is the position along the direction of permeation. The dq/dx is calculated using Langmuir constants, which are obtained from the results of the grand canonical ensemble Monte Carlo (GCMC) calculations. In the following calculations, dx was set to 1 μm. The dependence of transport diffusion coefficients on concentration is taken into account in eq 6. In eq 7, it is assumed that the amount of adsorption on both membrane surfaces reaches equilibrium immediately comparing with the intracrystalline diffusion rate of adsorbed species. As a result, there is no permeation resistance when a molecule permeates through the membrane. The influence of this surface resistance on diffusivity has been reported as the cause of the differences in diffusion coefficients obtained using several measurement methods.[22,25,28,29] However, the surface resistance is still obscure.

3. Simulations

An MFI type silicalite crystal structure used in this study is represented by the *Pnma* space group (orthorhombic), with lattice parameters $x = 20.022$ Å, $y = 19.899$ Å, $z = 13.383$ Å. The silicalite structure had two types of channels as shown in Figure 1: a straight channel parallel to the y direction and a zigzag channel running in the a direction. An MD and MC unit cell consisted of two unit cells superimposed along the z direction, and included 192 silicon and 384 oxygen atoms. A periodic boundary condition was applied to the unit cell. Sorbate loading in MD simulations were set at 1, 2, 4, 8, and 12 molecules/unit cell.

Cerius[2] version 3.5 code, supplied by MSI Inc., was used to carry out MD and MC calculations. We chose burchart 1.01-DREIDING2.21 as the force field set suitable for reproducing experimental results of the energetic properties of organic molecules on zeolite.[30] We considered bonding, angle, torsion, inversion, Urey−Bradley, and van der Waals interactions to describe the interatomic potential in the zeolite framework and adsorbed molecules. The electrostatic interaction was also used for atoms in the zeolite framework. The Ewald method was used for the summation of electrostatic interactions. The atomic charge of Si and O were +0.38e and −0.19e, respectively. Nonbonding interactions between adsorbed molecules and the zeolite framework were represented by the van der Waals interaction, the cutoff length for the nonbonding interactions being fixed at 8 Å. The rather short cutoff length was chosen to perform enough long MD calculation to obtain well-statistic properties, considering the restriction of computational cost. The error of the heat of adsorption due to this value was less than 4%. The thermal atomic motion of all atoms of the zeolite lattice and adsorbate molecules was considered in all MD calculations. The hydrogens in adsorbate molecules were modeled explicitly. An NVE ensemble (number of atoms in unit cell, volume, and total energy were kept constant) was used for the MD calculations, and a velocity corresponding to the Boltzmann distribution at 300 K was given to all atoms in an MD unit cell before performing the MD calculation. The average temperatures of all MD calculations were found in the range of ±8 K around 300 K. The integrated simulation time per single MD step was 1 fs. There were 300 000 simulations, which corresponds to 300 ps in real time. The last 200 000 steps were used for estimating the self-diffusion coefficient, which was calculated by a mean square displacement (MSD) of each atom of adsorbate with entailing an average over 40 of time origins, using the Einstein relationship.

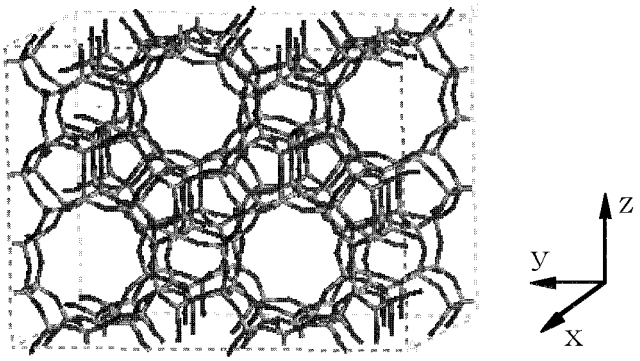

Figure 1. Schematic figure of MFI type silicalite. Zeolite framework bonding of Si and O atoms in a unit cell is shown.

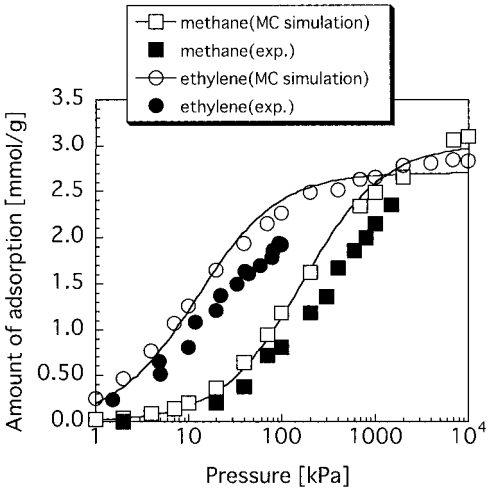

Figure 2. Adsorption isotherm for methane and ethylene in silicalite obtained by MC calculations. Available experimental data (refs 31 for methane and ref 32 for ethylene) are also presented. Solid lines represent the fitted result of the Langmuir curve.

TABLE 1: Heats of Adsorption of Methane and Ethylene in Silicalite at 300 K Obtained by MC Calculation and Available Experimental Data

	MC [kJ/mol]	exptl[10,31,38] [kJ/mol]
methane	22.1	18.1−22.5
ethylene	32.5	27

TABLE 2: Estimated Langmuir Parameters at 300 K from MC Results

	q_s [mmol/g]	b [kPa^{-1}]
methane	3.02	6.06×10^{-3}
ethylene	2.71	8.09×10^{-2}

GCMC simulations were carried out to determine the isotherms of methane and ethylene in silicalite using the same force field set. The total number of MC cycles was 500 000 steps, which was adequate for reaching equilibrium of the total energy and loading of the system. The last 300 000 steps were used in sampling for statistical analysis.

4. Results and Discussion

4.1. Equilibrium. Calculated adsorption isotherms and isosteric heats of adsorption are shown in Figure 2 and Table 1, together with the experimental data. It was found that calculated isotherms agreed with available experimental data. GCMC results of Langmuir parameters are shown in Table 2, where it can be seen that the adsorption isotherms show good agreement with the Langmuir curve over a wide pressure range. Both the isosteric heat of adsorption and the adsorption isotherm agree favorably with the experimental data. We therefore consider the force field of burchart 1.01-DREIDING2.21 to be suitable for representing the system of methane and ethylene in silicalite.

4.2 Dynamics. Figure 3 shows the molecular trajectories of methane in silicalite, obtained from MD calculations. It is shown that the region with the highest density of trajectories is located at the intersections of the straight and zigzag channels and at the channel segments. The high-density region is one where molecules remained for a long time, and the low-density region is where the diffusivity of molecules was significantly high. Thus, high-density regions are considered to be an adsorption site. A similar trajectory was also observed in the MD results of ethylene. The results imply that the adsorption−diffusion model can explain the diffusion of methane and ethylene in silicalite.

Calculated self-diffusion coefficients are shown in Figure 4, together with the experimental[34,35] and previous MD data.[10,36,37] It was found that self-diffusion coefficients steadily decreased as the loading increased, which is in good agreement with the presented experimental data. Figures 5 and 6 show the anisotropic self-diffusion coefficients of methane and ethylene, respectively. The dependence of self-diffusion coefficients on the loading is found in the *y* direction only for a range lower than 1.4 mmol/g. However, the self-diffusion coefficients in the *x* and *z* directions are independent of the loading. This phenomenon is specific for ethylene in silicalite. The diffusion coefficients in three directions, shown in Figure 6, have approximately the same values for a loading larger than 1.4 mmol/g.

This anisotropic diffusivity can be explained as follows. The molecular sizes were so close to the zigzag channel diameter that the diffusion behavior in the *x* and *z* directions was mainly governed by the interaction between the adsorbed molecule and channel wall. Consequently, the interaction between molecules was not significant, and the dependence of diffusion coefficients on the loading became small. In the diffusion through a straight channel that was expanding toward the *y* direction, the interaction between adsorbed molecules was significant, in addition to the interaction with the channel wall, because the channel diameter was large enough to diffuse. As a result, the diffusion coefficient in the *y*-direction became a function of the number of adsorbed molecules.

The calculated corrected diffusion coefficients are shown in Table 3. Figures 7 and 8 show the calculated transport-diffusion coefficients with self-diffusion coefficients of methane and ethylene, respectively. In the low-loading region, the values for self-diffusion and transport-diffusion coefficients are seen to come close to one another. However, in the high-loading region, transport diffusion coefficients increased rapidly and were much larger than self-diffusion coefficients. The self-diffusion coefficients of methane were larger than those of ethylene, as shown in Figure 4. In the high-loading region, however, the transport diffusion coefficients of methane were smaller than those of ethylene. This was due to the adsorption capacity of methane being greater than that of ethylene. Moreover, the contribution of the adsorption capacity became large in the high-loading region, as described in eq 3.

4.3 Permeability. The permeability of methane through a silicalite membrane was calculated using transport diffusion coefficients and Langmuir parameters, assuming that the adsorption−diffusion model could describe the diffusion of molecules.

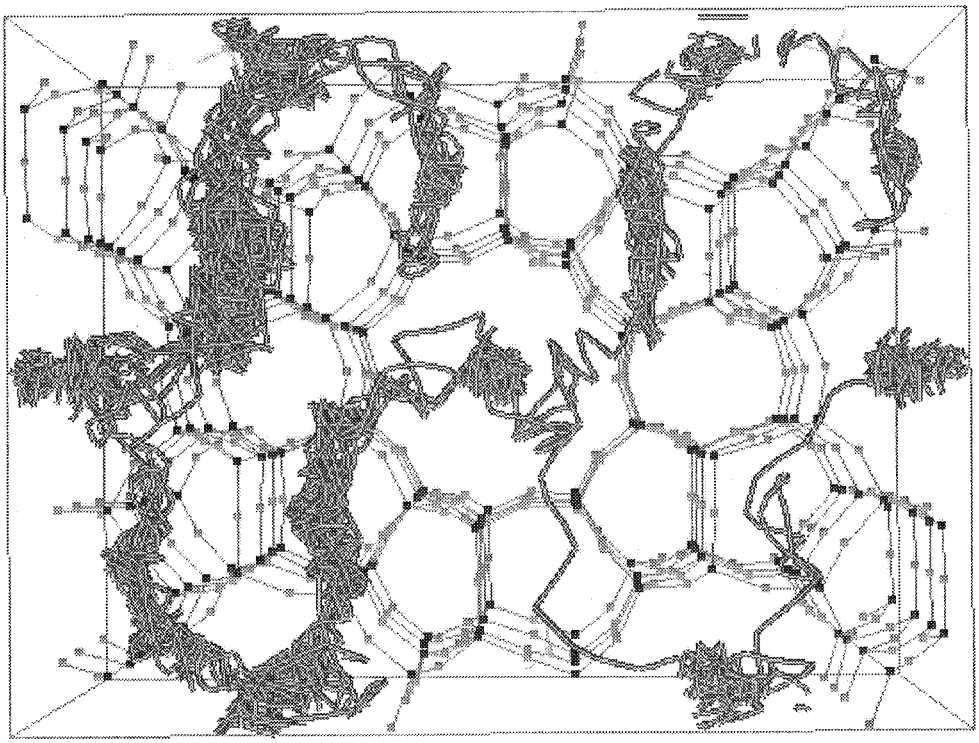

Figure 3. Molecular trajectories of methane in the silicalite, obtained from MD calculation. RYUGA code was used for drawing this figure.[33] The positions of carbon atom every 1 ps during 100 ps MD run are presented.

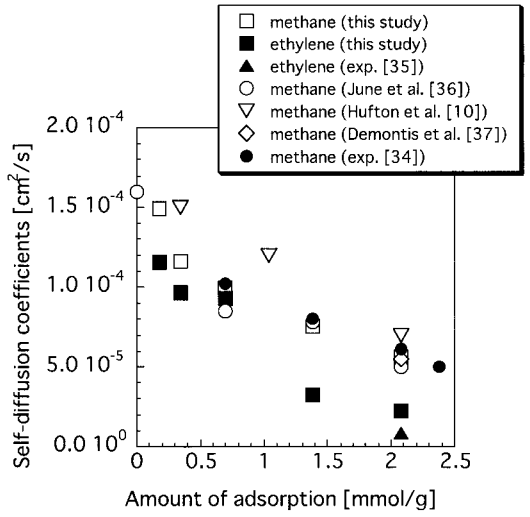

Figure 4. MD results of self-diffusion coefficients of methane and ethylene in silicalite, together with available experimental data.[34,35] Results of previous MD works[10,37,38] were also presented.

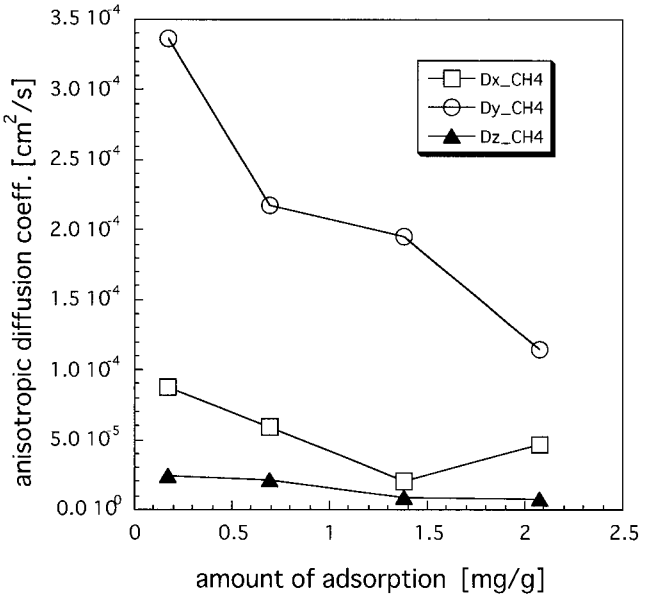

Figure 5. Calculated anisotropic self-diffusion coefficients of methane.

The conditions used in the following calculation, such as feed side-pressure and permeate side-pressure, are summarized in Table 4. The applied pressure of the feed gas was within the range where self-diffusion coefficients were in the correct proportion to the amount of adsorption to satisfy eq 3. The calculated permeabilities with experimental data[1,3,40,41,42] are shown in Table 5. Although there is a great deal of difference between the available experimental data, it was found that the calculated value was larger than the experimental values by at least an order of magnitude.

One plausible reason for this discrepancy lies in the structure of a membrane. The permeabilities shown in Table 5 were calculated using the value of membrane thickness. Almost all zeolite membranes are formed on the support layer, and it is difficult to measure correctly the thickness of the dense layer that contributes to separation of molecules. In addition, crystalline defects and the barrier effect of intergrowth on diffusivity were not included in the molecular simulations, although the experimental membranes seemed to possess intercrystalline defects that could result in the large difference in permeabilities. Permeation resistance is sometimes caused by the material of the support layer.[1,42] A resistance is associated with a difference in the concentrations of permeated species at the permeate side of the dense layer, and at the permeate side of the support layer. However, in the case of methane through a metal or alumina layer, the permeance through the support layer is 30−100 times larger than that through the membrane. Therefore, the resistance at the support layer is thought to be very small and so does not affect the permeability.

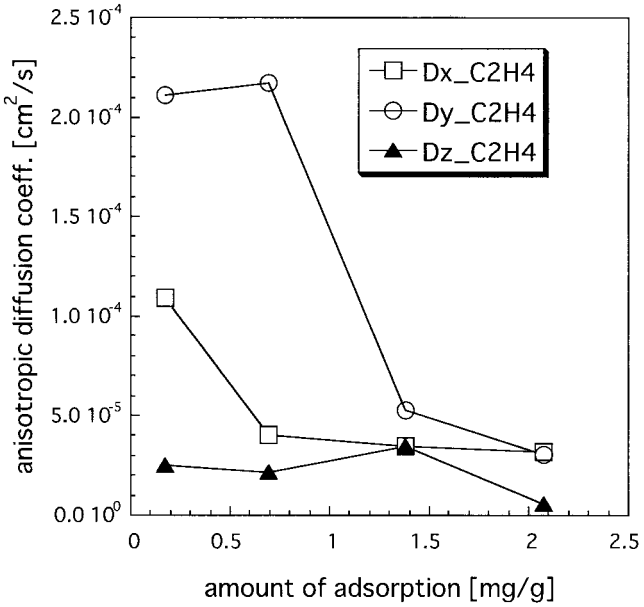

Figure 6. Calculated anisotropic self-diffusion coefficients of ethylene.

TABLE 3: Estimated Corrected Diffusivity D_0 from MC and MD Results Using Eq 3

	D_0 [cm²/s]
methane	1.4×10^{-4}
ethylene	1.2×10^{-4}

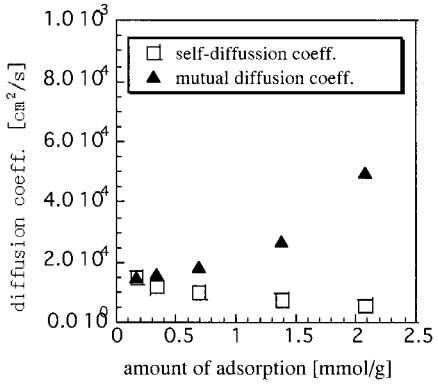

Figure 7. Calculated transport-diffusion coefficients with self-diffusion coefficients for methane in silicalite.

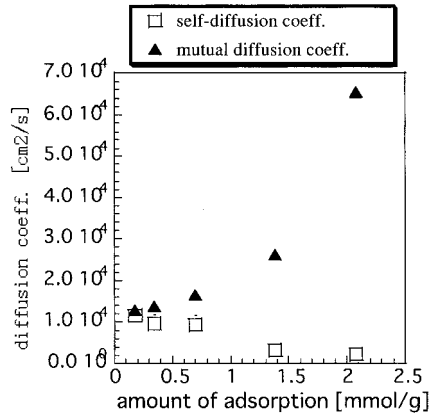

Figure 8. Calculated transport-diffusion coefficients with self-diffusion coefficients for ethylene in silicalite.

The adsorption−diffusion mechanism, used in the derivation of equations 1−6, assumes that permeation of each molecule is not influenced by the flow of another permeated molecule.

TABLE 4: Considered Condition for Calculation of Permeability of Methane and Ethylene through a Silicalite Membrane

membrane thickness	10 μm
gas pressure at feed side	100 kPa (methane) 10 kPa (ethylene)
gas pressure at permeated side	0 kPa

TABLE 5: Comparison of Calculated Permeabilities of Methane and Ethylene in Silicalite with Experimental Data

molecule	reference	permeability [$\times 10^{-10}$ cm³ (STP) cm/(cm² s Torr)]
methane	this study	1.1×10^5
	5,34[a]	6.4×10^4
	1,40[b]	$0.9 \times 10^2 - 2.1 \times 10^2$
	3,42[b]	$3.5 \times 10^3 - 6.0 \times 10^3$
	41[b]	$3.6 \times 10^3 - 1.6 \times 10^4$
ethylene	this study	1.0×10^6

[a] Permeability was calculated using experimental data. Experimental corrected diffusivity was obtained by PFG-NMR method,[34] while Langmuir parameters were taken from the isotherm in ref 5. [b] Permeability was measured by membrane technique.

TABLE 6: Calculated Anisotropic Permeabilities [$\times 10^{-10}$ cm³ (STP) cm/(cm² s Torr)]

	permeability		
direction	methane	methane[a]	ethylene
x	6.0×10^4	1.2×10^4	6.4×10^5
y	2.5×10^5	5.1×10^4	2.2×10^6
z	2.0×10^4	4.0×10^3	1.9×10^5
y		5.5×10^4 [11]	

[a] Calculation condition was the same as that reported by Pohl et al.,[11] where feed gas pressure was 20 000 kPa, while gas pressure at the permeated side was 150 kPa.

Fritzsche et al.[14] calculated the transport-diffusion and self-diffusion coefficients of methane through LTA type zeolite, using the GCMD method, and concluded that the viscous flow in zeolite should be ignored, because the two calculated diffusion coefficients strictly obey the Darken relationship. Their results support the validity of our assumption. Moreover, the feed gas pressure in the permeability calculations was small enough so that viscous flow in the zeolite pore could be disregarded.

The calculated anisotropic permeabilities are shown in Table 6. Differences of more than a factor of 10 are observed in the permeabilities along the *y* and *z* directions. These results mean that experimental permeabilities will differ greatly with the orientation of the membrane. In this study, permeability in the *z* direction was found to agree favorably with the available experimental data shown in Table 5. This agreement may suggest that the experimental membranes are highly oriented in the *y* direction. Moreover, permeability in the *y* direction was found to agree well with that obtained from the GCMD method reported by Pohl,[11] which simulated the permeation along the *y* direction. In our calculations, the adsorption/desorption processes were assumed to be much faster than the migration through the zeolite pores. In the case of methane in silicalite, there is a possibility that the adsorption rate at the membrane phase boundary causes the resistance of the permeation, because the diffusion coefficient of methane is large. The agreement of these permeabilities, calculated by two different methods, implies that there is no resistance at the membrane surfaces because, in the GCMD method, the surface resistance was an artifact of the simulation.

5. Conclusion

In this work, we have tried to illustrate the diffusion model for methane and ethylene in silicalite based on an adsorption−diffusion model. A theoretical equation was presented to predict the ideal permeability of the zeolite membrane. The MD method was used to obtain the self-diffusivities of methane and ethylene in zeolite, and the calculated self-diffusion coefficients agreed well with those of the experimental data. The MC method was used to calculate the isotherms in zeolite, and the calculated isotherms of methane and ethylene in silicalite agreed well with those of determined by experiment.

We estimated the permeabilities of methane and ethylene in silicalite, using the results obtained from MC and MD calculations. Assuming that D'_{1v} is proportional to the concentration of vacant adsorption sites, the relationship between self-diffusion coefficient and corrected diffusion coefficient was derived and used to estimate the permeability of a single component gas through the membrane. The calculated permeabilities differed from available permeability data by more than an order of magnitude; these differences may be due to the structural difference between our calculated model and that of the experiment, but a more detailed study is needed to clarify this point.

Calculated anisotropic permeability of methane and ethylene through silicalite indicated that the permeability along the *y* direction was larger, by a factor of 10, than those in other directions. This result highlights the importance of controlling the orientation of zeolite crystal in membrane design. The calculated permeability of methane along the *y* direction was consistent with the value calculated using the GCMD technique,[11] which simulated the flow along the *y* direction.

The presented methodology for the calculation of permeability is easily applied to the estimation of the dependence of permeability on gas pressure at the feed side or the permeated side, and on membrane thickness. This can be done without incurring the computational cost of MD and MC calculations. The great advantage is that the properties of a zeolite membrane can be understood quickly. This shows that molecular simulation methods are powerful tools in the design of a practical membrane.

References and Notes

(1) Vroon, Z. A. E. P.; Keizer, K.; Burggraaf, A. J.; Verweij, H. *J. Membr. Sci*. **1998**, *144*, 65−76.

(2) Bakker, W. J. W.; Kapteijn, F.; Poppe, J.; Moulijn, J. A. *J. Membrane Sci.* **1996**, *117*, 57−78.

(3) Coronas, J.; Noble, R. D.; Falconer, J. L. *Ind. Eng. Chem. Res.* **1998**, *137*, 166−176.

(4) Coronas, J.; Falconer, J. K.; Noble, R. D. *AIChE J*. **1997**, *43* (7), 1797−1812.

(5) Smit, B. *J. Phys. Chem.* **1995**, *99*, 5597−5603.

(6) June, R. L.; Bell, A. T.; Theodorou, D. N. *J. Phys. Chem*. **1990**, *94*, 1508−1516.

(7) Smit, B.; Daniel, L.; Loyens, J. C.; Verbist, G. L. M. M. *Faraday Discuss.* **1997**, *106*, 93−104.

(8) June, R. L.; Bell, A. T.; Theodorou, D. N. *J. Phys. Chem*. **1990**, *94*, 8232.

(9) Catlow, C. R. A.; Freeman, C. M.; Vessal, B.; Tomlinson, S. M.; Leslie, M. *J. Chem. Soc., Faraday Trans*. **1991**, *87*, 1947−1950.

(10) Hufton, J. R. *J. Phys. Chem.* **1991**, *95*, 8836−8839.

(11) Pohl, P. I.; Heffelfinger, G. S.; Smith, D. M. *Mol. Phys.* **1996**, *89* (6), 1725−1731.

(12) Maginn, E. J.; Bell, A. T.; Theodorou, D. N. *J. Phys. Chem*. **1993**, *97*, 4173−4181.

(13) Cracknell, R. F.; Nicholson, D.; Quirke, N. *Phys. Rev. Lett*. **1995**, *74*, 2463.

(14) Fritzsche, S.; Haberlandt, R.; Karger, J. *Z. Zeitschrift fur Physikalische* **1995**, *189*, S.211−220.

(15) Heffelfinger, G. S.; von Swol, F. *J. Chem. Phys*. **1994**, *100*, 7548−7552.

(16) MacElroy, J. M. D. *J. Chem. Phys*. **1994**, *101*, 5274−5280.

(17) Kapteijn, F.; Bakker, W. J. W.; Zheng, G.; Moulijn, J. A. *Microporous Materials* **1994**, *3*, 227−234.

(18) Vroon, Z. A. E. P.; Keizer, K.; Verweij, H.; Burggraaf, A. J. *J. Membr. Sci.* **1996**, *113*, 293−300.

(19) Krishna, R.; Smit, B.; Vlugt, T. J. H *J. Phys. Chem. A* **1998**, *102*, 7727−7730.

(20) Krishna, R.; Vlugt, T. J. H.; Smit, B. *Chem. Eng. Sci.* **1999**, *54*, 1751−1757.

(21) Fried, J. R.; Sadat-Akhavi, M.; Mark, J. E. *J. Membr. Sci.* **1998**, *149*, 115−126.

(22) Talu, O.; Shah, D. B.; Sun, M. S. *AIChE J*. **1998**, *44* (3), 681.

(23) Heink, W.; Karger, J.; Pfeifer, H.; Datema, K. P.; Nowak, A. K. *J. Chem. Soc., Faraday Trans.* **1992**, *88*, 3505−3509.

(24) Geus, E. R.; Bekkum, H. V.; Bakker, W. J. W.; Moulijn, J. A. *Microporous Materials* **1993**, *1*, 131−147.

(25) Kärger, J.; Ruthven, D. M. *Diffusion in Zeolite and Micropourous Solids*; Wiley-Interscience: New York, 1992.

(26) Krishna, R. *Gas Sep. Pur*. **1993**, *7* (2), 91.

(27) Krishna, R.; Wesselingh, J. A. *Chem. Eng. Sci.* **1997**, *52* (6), 861−911.

(28) Runnebaum, R, C.; Maginn, E. J. *J. Phys. Chem. B* **1997**, *101*, 6394−6408.

(29) Kärger, J.; Ruthven, D. M. *ZEOLITES* **1989**, *9*, 267.

(30) Manual of Cerius 2, version 3.5, supplied by Molecular Simulation Inc., 1997.

(31) Abdul-Rehman, H. B.; Hasanain, M. A.; Loughlin, K. F. *Ind. Eng. Chem. Res*. **1990**, *29*, 1525−1535.

(32) Kapteijn, F.; Bakker, W. J. W.; Zheng, G.; Poppe, J.; Moulijn, J. A. *Chem. Eng. J*. **1995**, *57*, 145−153.

(33) Miura, R.; Yamano, H.; Yamauchi. Y.; Kubo, M.; Miyamoto, A *Catal. Today* **1995**, *23*, 409−416.

(34) Caro, J.; Bülow, M.; Shirmer, W.; Kärger, J.; Heink, J.; Pfeifer, H. *J. Chem. Soc., Faraday Trans.* **1985**, *81*, 2541.

(35) Snurr, R. Q.; Hagen, A.; Ernst, H.; Schwarz, H. B.; Ernst, S.; Weitkamp, J.; Kärger, J. *J. Catal*. **1996**, *163*, 130−137.

(36) June, R. L.; Bell, A. T.; Theodorou, D. N. *J. Phys. Chem*. **1990**, *94*, 8232−8240.

(37) Demontis, P.; Suffritti, G. B.; Fois, E. S.; Quartieri, S *J. Phys. Chem*. **1992**, *96*, 1482−1490.

(38) Rees, L. V. C.; Brückner, P.; Hampson, J. *Gas Sep. Purif.* **1991**, *5*, 67.

(39) Burggraaf, A. J.; Vroon, Z. A. E. P.; Keizer, K.; Verweij, H. *J. Membr. Sci.* **1998**, *144*, 77−86.

(40) Bakker, W. J. W.; Broeke, L. J. P. V. D.; Kapteijn, F.; Moulijn, J. A. *AIChE J*. **1997**, *43* (9), 2203.

(41) Graaf, J. M. V. D.; Kapteijn, F.; Moulijn, J. A. *J. Membr. Sci.* **1998**, *144*, 87−104.

(42) Funke, H. H.; Kovalchick, M. G.; Falconer, J. L.; Noble, R. D. *Ind. Eng. Chem. Res.* **1996**, *35*, 1575−1582.